Bull. Mater. Sci., Vol. 38, No. 7, December 2015, pp. 1757–1764. © Indian Academy of Sciences.

Synthesis of MgAl-LDH/$CoFe_2O_4$ and MgAl-CLDH/$CoFe_2O_4$ nanofibres for the removal of Congo Red from aqueous solution

ZHIGANG JIA*, SHENGBIAO LI, JIANHONG LIU, QI QIN and RONGSUN ZHU
School of Chemistry and Chemical Engineering, Anhui University of Technology, Ma'anshan 243002, Anhui Province, PR China

MS received 8 November 2014; accepted 10 August 2015

Abstract. **MgAl-LDH/$CoFe_2O_4$ and MgAl-CLDH/$CoFe_2O_4$ nanofibres were prepared by urea-hydrolysed hydrothermal reaction and the subsequent calcinations. The morphology and structure of the products were characterized by X-ray diffraction, scanning electron microscopy and transmission electron microscope and Fourier transformed infrared. The adsorption performance of MgAl-LDH/$CoFe_2O_4$ and MgAl-CLDH/$CoFe_2O_4$ nanofibres for the removal of an anionic dye (Congo Red, CR) from aqueous solution was investigated. The results showed that MgAl-LDH/$CoFe_2O_4$ and MgAl-CLDH/$CoFe_2O_4$ nanofibres are particularly efficient in removing CR. The adsorption follows a pseudo-second-order kinetic model and best fits the Langmuir isotherm model. The maximum adsorption capacities of MgAl-LDH/$CoFe_2O_4$ and MgAl-CLDH/$CoFe_2O_4$ nanofibres for CR were found to be 213.2 and 49.8 mg g^{-1}, respectively. The both adsorption processes were found to be spontaneous and exothermic in nature.**

Keywords. **Cobalt ferrite; layered double hydroxide; adsorption; Congo Red.**

1. Introduction

Controlling pollution is the main concern of society today. Dye contamination in industrial wastewater, resulting from textiles, paper, printing, plastics, leather and so on, has become one of the most serious environmental problems worldwide.[1] About 15% of the total world production of dyes is lost during the dyeing process and is released in textile effluents.[2] Textile industry wastewater contains a wide variety of dyes, which are hardly chemically decomposed and may be transmuted to toxic compounds harmful to ecosystem and human being.[3] Due to their low biodegradability, various methods have been developed to eliminate the organic pollutants, such as chemical oxidation, microbial degradation, adsorption, flocculation and photocatalytic degradation.[4] Among these, adsorption is considered to be superior to other approaches because of its high efficiency and low cost to wastewater treatment.[5]

LDH with highly positive surface charge, low cost and large surface area has been demonstrated as good adsorbents to effectively remove acidic or negatively charged compounds such as organic dyes.[6,7] However, as using LDH for removal of dye, separation becomes a difficult and time-consuming process.[8] A possible solution could be the development of absorbent with magnetic matrix, allowing easy separation of the absorbent by simply applying an external magnetic field.[9,10]

Magnetic composites have received increasing attention in the past few decades because of their unique properties and potential applications in various fields.[11] In this study, batch type experiments were carried out to investigate the capacity of MgAl-LDH/$CoFe_2O_4$ and MgAl-CLDH/$CoFe_2O_4$ nanofibres for adsorption of CR reactive dye. The effects of some parameters such as dye concentration, adsorbent weight and temperature on the adsorption process were separately investigated. The fitting of the obtained adsorption isotherms to the Langmuir and Freundlich models is also studied to explain the adsorption of the reactive dye on MgAl-LDH/$CoFe_2O_4$ and MgAl-CLDH/$CoFe_2O_4$ nanofibres.

2. Experimental

2.1 *Chemicals*

Analytical grade cobalt sulphate ($CoSO_4{\cdot}7H_2O$), ammonium ferrous sulphate ($FeSO_4{\cdot}(NH_4)_2SO_4{\cdot}6H_2O$), oxalic acid dihydrate ($H_2C_2O_4{\cdot}2H_2O$), magnesium nitrate ($Mg(NO_3)_2{\cdot}6H_2O$), aluminium nitrate ($Al(NO_3)_3{\cdot}9H_2O$) and urea ($CO(NH_2)_2$) were utilized to prepare MgAl-LDH/$CoFe_2O_4$ nanofibres without further treatment.

2.2 *Materials synthesis*

2.2a *Synthesis of $CoFe_2O_4$ nanofibres*: $CoFe_2O_4$ nanofibres were prepared by a hydrothermal route according to Zhigang Jia's method with a minor modification.[12] The synthesis of $CoFe_2O_4$ was conducted in two steps: the hydrothermal synthesis and calcine of iron-cobalt oxalate precursor. First of all, two kinds of solution were prepared. Solution 1: 0.562 g

*Author for correspondence (zjchemyue@126.com)

$CoSO_4{\cdot}7H_2O$ and 1.568 g $FeSO_4{\cdot}(NH_4)_2SO_4{\cdot}6H_2O$ were dissolved in 40 ml glycol and water mixed solution with the glycol/water volume ratio of 3. Solution 2: 0.908 g $H_2C_2O_4{\cdot}2H_2O$ was dissolved in 40 ml mixed solution with the same proportion. Then, solution 1 was added slowly into solution 2 with vigorous stirring and mixed for 5 min and the final slurry was obtained. Second, the final slurry was put into the Erlenmeyer flask (250 ml) and heated at 120°C for 24 h. Then the product was filtered and washed with deionized water for several times, and the obtained iron-cobalt oxalate precursor was dried at 80°C for 4 h. The $CoFe_2O_4$ nanofibres were obtained by calcination in air at 600°C for 2 h.

2.2b *Synthesis of MgAl-LDH/$CoFe_2O_4$ and MgAl-CLDH/$CoFe_2O_4$ nanofibres*: The LDH/$CoFe_2O_4$ nanofibres were synthesized by a hydrothermal route under urea hydrolysis. A typical synthetic procedure was as follows: 0.1 g of dried $CoFe_2O_4$ nanofibres was added into 50 ml deionized water with ultrasonication for 10 min. $Al(NO_3)_3{\cdot}9H_2O$ (0.056 g), $Mg(NO_3)_2{\cdot}6H_2O$ (0.077 g) and $CO(NH_2)_2$ (0.09 g) were added into the above suspension and then sonicated for 10 min. Subsequently, the mixed solution was transferred into reactor (250 ml) and heated at 100°C for 24 h. After cooling to room temperature, the resulting black precipitate was collected by magnetic separation, washed with deionized water several times and dried at 45°C under vacuum overnight. The MgAl-CLDH/$CoFe_2O_4$ nanofibres were obtained by calcination in air at 500°C for 4 h and placed in a desiccator for the following experiments.

2.3 *Characterization*

XRD patterns were obtained with a D8 Advance diffractometer using CuKα radiation. Scanning electron microscope (SEM) images were obtained on a JSM-6360LV. Transmission electron microscopy (TEM) images were obtained on a Philips Tecnai F20 instrument working at 200 kV. The Fourier transformed infrared (FTIR) spectroscopy of the samples was recorded in the wavenumber range of 400–4000 cm^{-1} by means of the Thermo Nicolet 6700 using KBr-powder mixed pellets.

2.4 *Adsorption experiments*

The adsorption properties of MgAl-LDH/$CoFe_2O_4$ and MgAl-CLDH/$CoFe_2O_4$ nanofibres as adsorbent for CR were studied by a batch adsorption experiment at various temperatures (298, 308 and 318 K), in which 10 mg of the adsorbent and 50 ml of the CR solutions (10–120 mg l^{-1}) was added. The stock solution of Congo Red (CR, chemical formula = $C_{32}H_{22}N_6Na_2O_6S_2$, FW = 696.68, λ_{max} = 497 nm; 1 g l^{-1}) was prepared in deionized water, and the required concentrations of the dye were got by diluting the stock solution with deionized water.[13] The absorbance value of the CR solutions was analysed by 721 spectrophotometer (Shanghai Precision & Scientific Instrument Co. Ltd, China) at λ_{max} = 497 nm. All experiments were repeated three times unless otherwise indicated.

By measuring the absorbance of different concentrations of the CR solutions, the adsorption capacity was evaluated on the basis of a mass balance between the initial and intermediate or final CR concentrations. The changes in the absorbance of all solution samples were presented and determined at certain time intervals during the adsorption process. The amount of CR adsorbed at equilibrium q_e (mg g^{-1}) was obtained by the following equation:

$$q_e = (C_0 - C_e)V/m, \tag{1}$$

where C_0 (mg g^{-1}) is the initial concentrations of CR solution, C_e (mg l^{-1}) the equilibrium concentrations of CR solution, V (l) the volume of the solution and m (g) the mass of the adsorbent.

Further, at t time, the quantity of CR adsorbed q_t (mg g^{-1}) was calculated by the following equation:

$$q_t = (C_0 - C_t)V/m, \tag{2}$$

where C_t (mg l^{-1}) is the CR concentration at t time. Then, kinetic studies were carried out on the adsorption of CR by as-synthesized nanofibres.

3. Results and discussions

3.1 *Morphology and structures of as-prepared adsorbents*

In our study, MgAl-LDH/$CoFe_2O_4$ nanofibres were first prepared by urea-hydrolysed hydrothermal reaction. Hydrothermal hydrolysis of urea was used to induce homogeneous precipitation of soluble metal salts for preparing highly crystalline MgAl-LDHs on the surface of $CoFe_2O_4$, which simultaneously provided a substrate for *in situ* growth of LDH.

Figure 1 shows the XRD patterns of $CoFe_2O_4$, MgAl-LDH/$CoFe_2O_4$ and MgAl-LDH/$CoFe_2O_4$ samples, respectively. In figure 1a, the diffraction peaks at 2θ = 18.7°, 30.0°, 35.6°, 43.1°, 57.0° and 62.6° (figure 1a) could be assigned to the (111), (220), (311), (400), (511) and (440) planes of $CoFe_2O_4$ phase,[14] which were in good agreement with the characteristic peaks of the standard compound $CoFe_2O_4$ (JCPDS: 22-1086). As seen from figure 1b, the main peak at 2θ = 30.1°, 35.4°, 43.2° fitted very well with those of pure $CoFe_2O_4$. Simultaneously, the diffraction peaks at 2θ = 11.6° and 22.3° could be assigned to the (003) and (006) planes of MgAl-LDH nanostructures.[15] However, the relatively weak intensity of the peaks of MgAl-LDH manifested a low crystallinity of LDH crystals in the as-prepared materials. The XRD pattern of the calcined MgAl-LDH/$CoFe_2O_4$ (figure 1c) showed that the characteristic peaks of MgAl-LDH disappeared and the characteristic peak of calcined MgAl-LDH were observed at 2θ = 43.2°, suggesting that the structure of MgAl-LDH/$CoFe_2O_4$ was destroyed when heated at 500°C due to decomposition of original LDH into

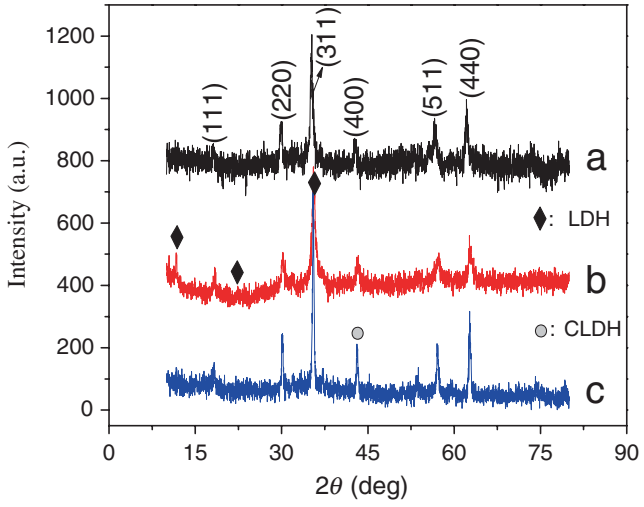

Figure 1. XRD patterns of (**a**) $CoFe_2O_4$, (**b**) MgAl-LDH/$CoFe_2O_4$ and (**c**) MgAl-CLDH/$CoFe_2O_4$ nanofibres.

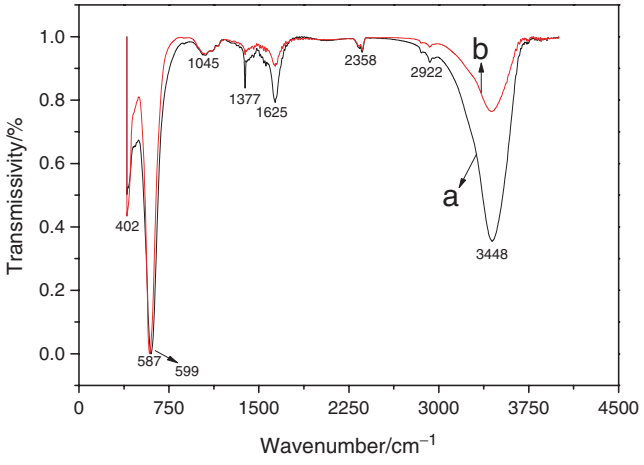

Figure 2. Fourier transformed infrared (FT-IR) spectra of (**a**) MgAl-LDH/$CoFe_2O_4$ and (**b**) MgAl-CLDH/$CoFe_2O_4$ nanofibres.

the mixed oxide of magnesium and aluminium during the calcination process.[16]

FT-IR spectra of MgAl-LDH/$CoFe_2O_4$ and calcined MgAl-LDH/$CoFe_2O_4$ are shown in figure 2. The spectrum of MgAl-LDH/$CoFe_2O_4$ in figure 2a shows the characteristic absorption bands of a hydroxyl group, particularly a broad band at 3448 cm^{-1} (due to the interlayer water molecules) with a shoulder near 2922 cm^{-1} (due to the H-banded stretching vibration). Weak bands at 2358 and 1625 cm^{-1} could be assigned to the H_2O bending vibration of interlayer water. The band at 1377 and 1045 cm^{-1} was assigned to the vibration of carbonate species.[17] Bands in the range of 600 cm^{-1} were attributed to metal-oxygen-metal stretching.[18] The spectrum of calcined MgAl-LDH/$CoFe_2O_4$ in figure 2b shows relatively weak band at 1377 and 3448 cm^{-1}, suggesting that the layered structure of MgAl-LDH in the composite destroyed during the calcination.

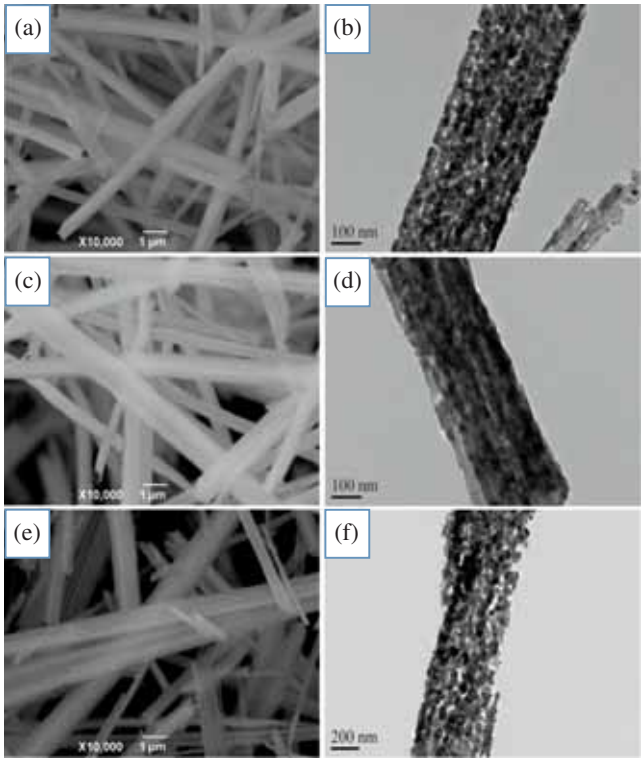

Figure 3. Scanning electron microscope and transmission electron microscope photographs of (**a**, **b**) $CoFe_2O_4$, (**c**, **d**) MgAl-LDH/$CoFe_2O_4$ and (**e**, **f**) MgAl-CLDH/$CoFe_2O_4$.

SEM and TEM were performed to examine the morphology of $CoFe_2O_4$, MgAl-LDH/$CoFe_2O_4$ and MgAl-CLDH/$CoFe_2O_4$, respectively. As shown in figure 3a, the as-prepared $CoFe_2O_4$ samples were fibres with high quality in terms of size, uniformity and crystallinity, which is similar to our previous reports. TEM image showed that the fibres were built by nanoparticles and holes can be clearly seen in figure 3b. Compared to the original $CoFe_2O_4$ nanofibres, MgAl-LDH/$CoFe_2O_4$ nanofibres exhibited much coarse surface (figure 3c) and holes were reduced as shown in figure 3d. During the hydrothermal procedure, the $CoFe_2O_4$ nanofibres acted as matrixes to adsorb metallic ions, followed by the nucleation and growth of the LDH crystallites. Therefore, the formation of LDH crystallites resulted in the reduction of holes of MgAl-LDH/$CoFe_2O_4$ nanofibres. However, the calcined MgAl-LDH/$CoFe_2O_4$ nanofibres (figure 3e and f) revealed obvious holes due to the decomposition of MgAl-LDH in MgAl-LDH/$CoFe_2O_4$ nanofibres, indicating that MgAl-LDH in the composite was converted into mixed magnesium and aluminium oxides.

3.2 *Adsorption kinetics*

The as-prepared MgAl-LDH/$CoFe_2O_4$ nanofibres were employed to remove the anion dye because of higher isoelectric point.[19] Figure 4 shows the effect of contact time on the adsorption capacity of CR onto MgAl-LDH/$CoFe_2O_4$ (a) and MgAl-CLDH/$CoFe_2O_4$ (b) nanofibres with different initial

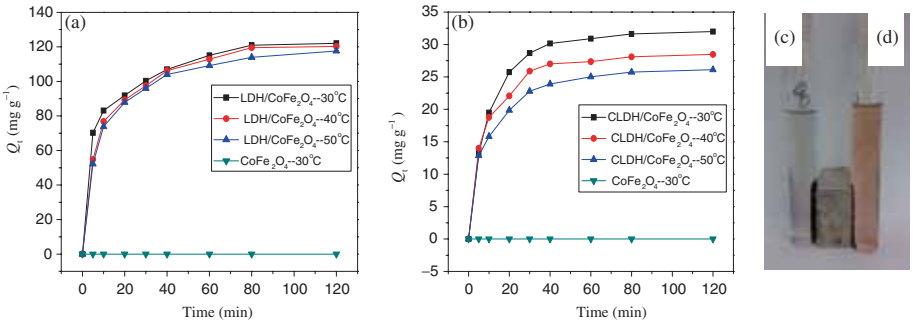

Figure 4. Effect of contact time for the adsorption of CR onto (**a**) MgAl-LDH/$CoFe_2O_4$ and (**b**) MgAl-CLDH/$CoFe_2O_4$ nanofibres with different temperature; (**c**) photos of separation of MgAl-LDH/$CoFe_2O_4$ and (**d**) MgAl-CLDH/$CoFe_2O_4$ nanofibres after adsorption by a magnet.

concentrations. It can be seen from figure 4a that the adsorption of CR onto MgAl-LDH/$CoFe_2O_4$ is quickly within a contact time of about 40 min and then increases further but slowly afterward. Equilibrium adsorption was achieved after approximately 80 min. The adsorption process of calcined MgAl-LDH/$CoFe_2O_4$ (as shown in figure 4b) was similar to the MgAl-LDH/$CoFe_2O_4$ nanofibres. The initial fast-adsorption could be a process predominated by memory effect of calcined MgAl-LDH/$CoFe_2O_4$ nanofibres, then it required a long time to reach the equilibrium. Compared with the MgAl-LDH/$CoFe_2O_4$ nanofibres, the MgAl-CLDH/$CoFe_2O_4$ nanofibres provided lower adsorption capacity. Furthermore, the MgAl-LDH/$CoFe_2O_4$ (figure 4c) and MgAl-CLDH/$CoFe_2O_4$ (figure 4d) after the adsorption of CR with an initial concentration of 20 mg l^{-1} and at 30 min can be quickly separated by a magnet, which leaves the clear solution behind as shown in figure 4. However, no adsorption of CR can be found for the $CoFe_2O_4$ nanofibres without the coating of LDH, indicating the LDH coating of MgAl-LDH/$CoFe_2O_4$ composite is responsible for the occurrence of adsorption.

Adsorption kinetics describes the rate of uptake of a dye by the adsorbent material.[20] The rate of dye removal from the water by the adsorbents can be evaluated by different kinetic models. Here, Lagergren pseudo-first-order and pseudo-second-order models are used to analyse the experimental data. These are the models most frequently used to describe the adsorption in solid–liquid systems.[21]

The Lagergren pseudo-first-order model is described by the following equation:

$$\ln\ (q_e - q_t) = \ln q_e - k_1 t, \tag{3}$$

where k_1 (min^{-1}) is the rate constant for pseudo-first-order adsorption kinetics. The values of k_1 and q_e for MgAl-LDH/$CoFe_2O_4$ (a) and MgAl-CLDH/$CoFe_2O_4$ (b) nanofibres can be calculated from the plot of ln (q_e–q_t) *vs.* t (in figure 5a and b), respectively.

The pseudo-second-order model is expressed as follows:

$$t/q_t = 1/k_2 {q_e}^2 + t/q_e, \tag{4}$$

where k_2 (g mg^{-1} min^{-1}) is the rate constant for pseudo-second-order adsorption kinetics. Values of q_e and k_2 for MgAl-LDH/$CoFe_2O_4$ (c) and MgAl-CLDH/$CoFe_2O_4$ (d) nanofibres are calculated from the intercept and slope by the linear plot of t/q_t *vs.* t (in figure 5c and d), respectively.

Table 1 shows the calculated kinetics parameters for MgAl-LDH/$CoFe_2O_4$ and MgAl-CLDH/$CoFe_2O_4$ nanofibres by pseudo-first-order and pseudo-second-order models. Here, a good agreement between calculated values q_e and the experimental ones $q_{e,exp}$ for MgAl-LDH/$CoFe_2O_4$ nanofibres is obtained by the linear plots of t/q_t *vs.* t (pseudo-second-order kinetic model). Whereas, the corresponding values q_e obtained from the pseudo-first-order model are much lower than the experimental data. Moreover, from the parameters listed in table 1, the correlation coefficients of the pseudo-second-order model ($R^2 > 0.99$) are much higher than those of the pseudo-first-order model. All these indicate that the adsorption process of MgAl-LDH/$CoFe_2O_4$ nanofibres best fits to the pseudo-second-order kinetic model. The adsorption process of MgAl-CLDH/$CoFe_2O_4$ nanofibres was similar to the former and also best fits to the pseudo-second-order kinetic model.

3.3 *Adsorption isotherms*

To describe the specific relation between the concentration of CR and the adsorption capacity of MgAl-LDH/$CoFe_2O_4$ and MgAl-CLDH/$CoFe_2O_4$ nanofibres, the adsorption isotherms are studied. Figure 6 shows the adsorption isotherms of CR adsorption onto MgAl-LDH/$CoFe_2O_4$ (a) and MgAl-CLDH/$CoFe_2O_4$ (b) nanofibres. From figure 6a, it can be seen that higher temperature was not favourable for the adsorption of CR onto MgAl-LDH/$CoFe_2O_4$ nanofibres, which showed an exothermic adsorption. This might be due to the physical bonding between acid dye molecules and the active sites of the adsorbent. Higher temperature weakens the interaction force of CR and MgAl-LDH/$CoFe_2O_4$ nanofibres. Figure 6b shows the adsorption isotherms of CR adsorption onto MgAl-CLDH/$CoFe_2O_4$ nanofibres. It can be seen that the adsorption capacity of MgAl-CLDH/$CoFe_2O_4$

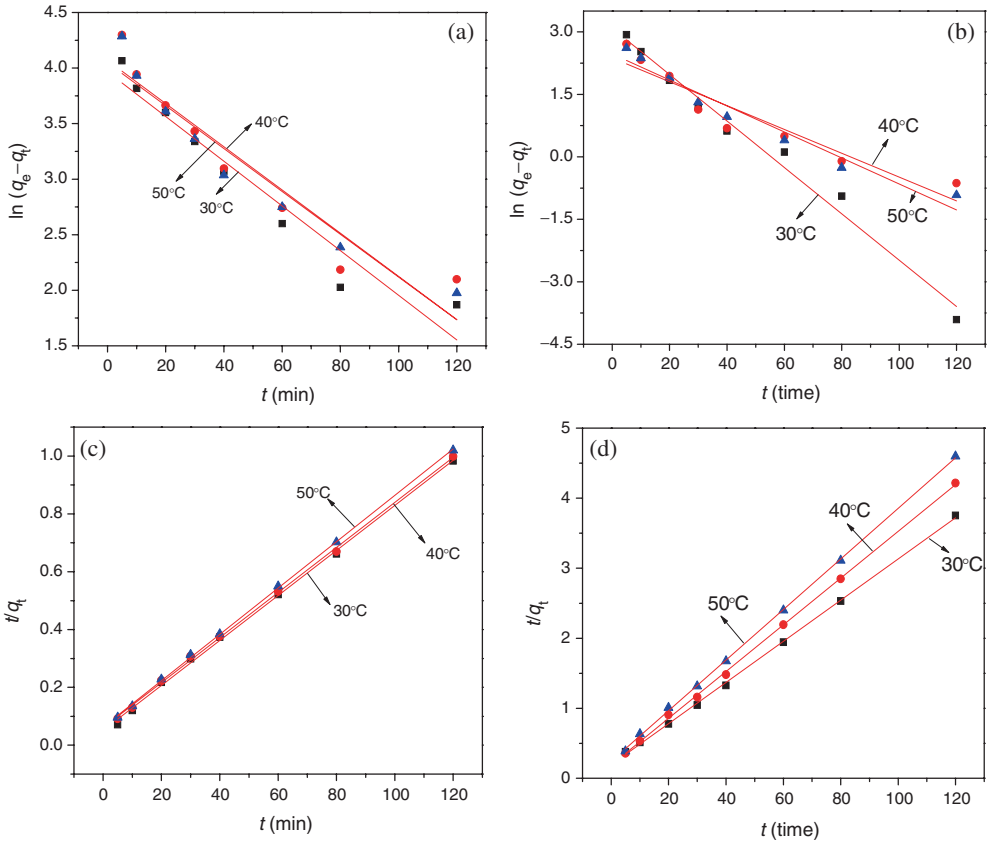

Figure 5. First-order kinetic plots of CR onto (**a**) MgAl-LDH/$CoFe_2O_4$ and (**b**) MgAl-CLDH/$CoFe_2O_4$ nanofibres; pseudo-second-order kinetic plots of CR onto (**c**) MgAl-LDH/$CoFe_2O_4$ and (**d**) MgAl-CLDH/$CoFe_2O_4$ nanofibres.

Table 1. Kinetics parameters for adsorption of MgAl-LDH/$CoFe_2O_4$ and MgAl-CLDH/$CoFe_2O_4$ nanofibres.

	Pseudo-first-order			Pseudo-second-order		
Temperature (°C)	k_1	q_e	R^2	k_2	q_e	R^2
MgAl-LDH/ $CoFe_2O_4$ nanofibres						
30	0.0201	52.8099	0.8605	0.0012	128.543	0.9962
40	0.0194	58.5341	0.7948	0.0009	128.369	0.9977
50	0.0193	57.2575	0.8529	0.0010	124.843	0.9990
MgAl-LDO/ $CoFe_2O_4$ nanofibres						
30	0.0557	21.9647	0.9623	0.0044	34.0251	0.9984
40	0.0285	10.7377	0.7787	0.0059	29.9490	0.9988
50	0.0312	11.8356	0.9009	0.0053	27.6778	0.9971

nanofibres increased with the increasing equilibrium concentration of CR. This could be due to the increasing driving force to overcome the mass transfer resistance of the adsorbate between the aqueous phases and the solid phases in case of higher concentrations. On the basis of the experimental data of CR adsorption onto MgAl-LDH/$CoFe_2O_4$ and MgAl-CLDH/$CoFe_2O_4$ nanofibres, the Langmuir and Freundlich isotherms are used to analyse how CR molecules interact with the adsorbents surface. Here, seven different concentrations (10, 20, 30, 40, 60, 80 and 120 mg l^{-1}) of CR are considered.

According to the assumption of adsorption on a homogeneous surface, a monolayer adsorption is described by the Langmuir model, where all sorption sites are identical and energetically equivalent. Then, the Langmuir isotherm can be expressed as

$$C_e/q_e = C_e/q_{max} + 1/k_l q_{max}\,, \tag{5}$$

where q_{max} (mg g^{-1}) is the maximum monolayer adsorption capacity, and k_l (l mg^{-1}) is a constant related to the energy of adsorption. The values of k_l and q_{max} of

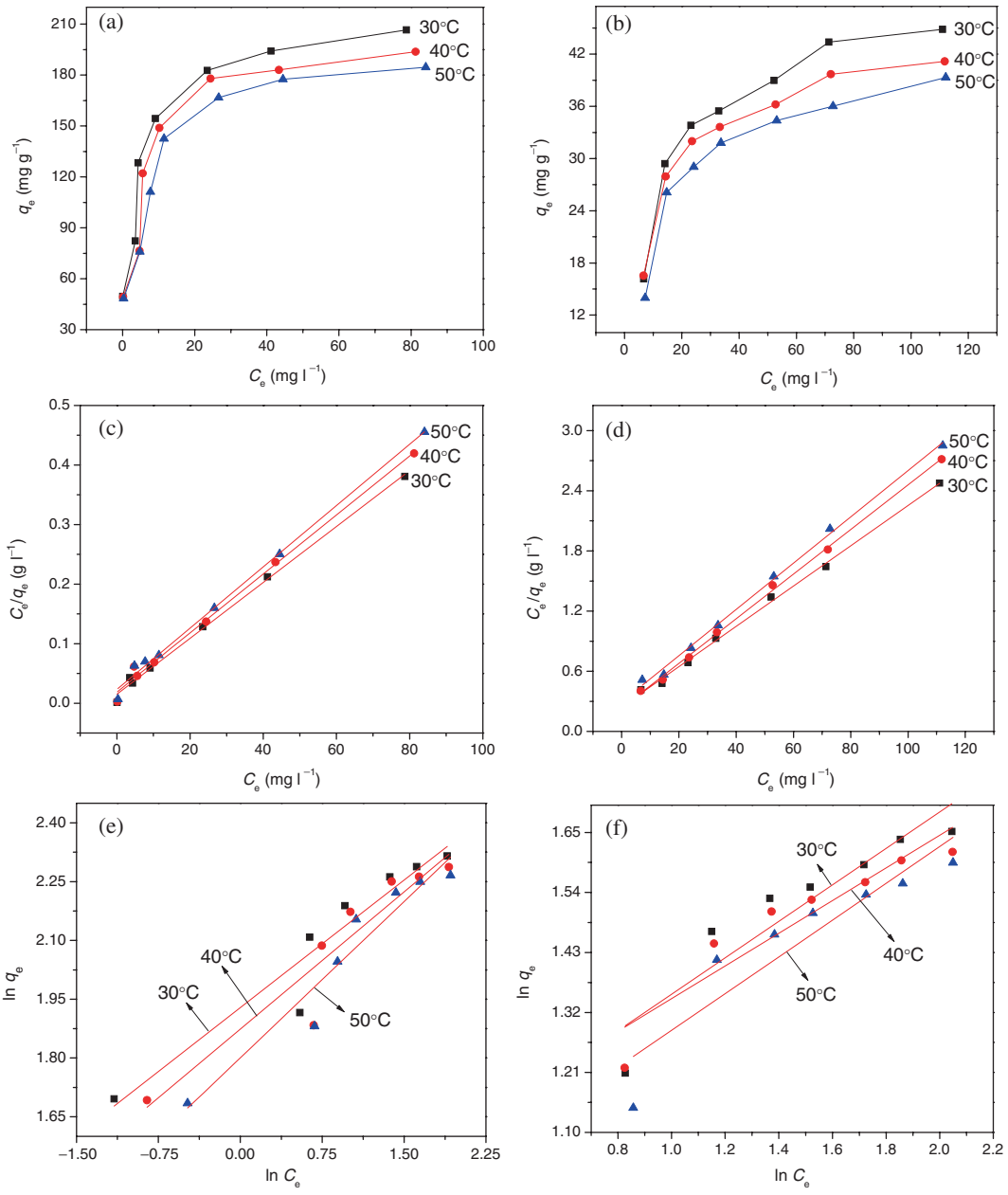

Figure 6. Adsorption isotherm for the adsorption of CR onto (**a**) MgAl-LDH/$CoFe_2O_4$ and (**b**) MgAl-CLDH/$CoFe_2O_4$ nanofibres; Langmuir plots for the adsorption of CR onto (**c**) MgAl-LDH/$CoFe_2O_4$ and (**d**) MgAl-CLDH/$CoFe_2O_4$ nanofibres; Freundlich plots for the adsorption of CR onto (**e**) MgAl-LDH/$CoFe_2O_4$ and (**f**) MgAl-CLDH/$CoFe_2O_4$ nanofibres.

MgAl-LDH/$CoFe_2O_4$ and MgAl-CLDH/$CoFe_2O_4$ were calculated from the slope and intercept of the linear plot C_e/q_e *vs.* C_e (as shown in figure 6c and d), respectively.

As to the Freundlich isotherm, the heterogeneous system is described, which does not restrict to the monolayer formations. A linear form of the Freundlich model can be expressed as the following equation

$$\text{Log } q_e = \log\ k_f + (1/n) \log\ C_e, \tag{6}$$

where k_f is the Freundlich equilibrium constant indicative of adsorption, $1/n$ is the Freundlich adsorption constant, the reciprocal of which is indicative of adsorption constant. The values of k_F and $1/n$ of MgAl-LDH/$CoFe_2O_4$ and MgAl-CLDH/$CoFe_2O_4$ can be calculated from intercept and slope of the linear plot between log C_e and log q_e (as shown in figure 6e and f). Also, a good adsorption process can be confirmed by the values of n ranging from 1.0 to 10.0.

Table 2 lists the calculated values from the Langmuir and Freundlich isothermal of the adsorption parameters for the CR adsorption onto MgAl-LDH/$CoFe_2O_4$ and MgAl-CLDH/$CoFe_2O_4$ nanofibres. Meanwhile, the correlation coefficients of MgAl-LDH/$CoFe_2O_4$ nanofibres calculated

Table 2. Isotherm parameters for adsorption of CR onto MgAl-LDH/$CoFe_2O_4$ and MgAl-CLDH/$CoFe_2O_4$ nanofibres.

	Langmuir constants			Freundlich constants		
Temperature (K)	q_m (mg g^{-1})	k_l (l mg^{-1})	R^2	k_f (mg g^{-1})	n (l mg^{-1})	R^2
MgAl-LDH/ $CoFe_2O_4$						
303	213.21	0.3099	0.9919	84.8008	4.6061	0.8240
313	202.02	0.2631	0.9872	74.7308	4.2808	0.7663
323	194.17	0.2224	0.9898	63.1247	3.7608	0.8431
MgAl-LDO/ $CoFe_2O_4$						
303	49.82	0.0818	0.9842	10.4488	2.9911	0.7113
313	44.94	0.0952	0.9967	11.1104	3.3372	0.7279
323	43.32	0.0786	0.9933	8.9166	2.9675	0.6746

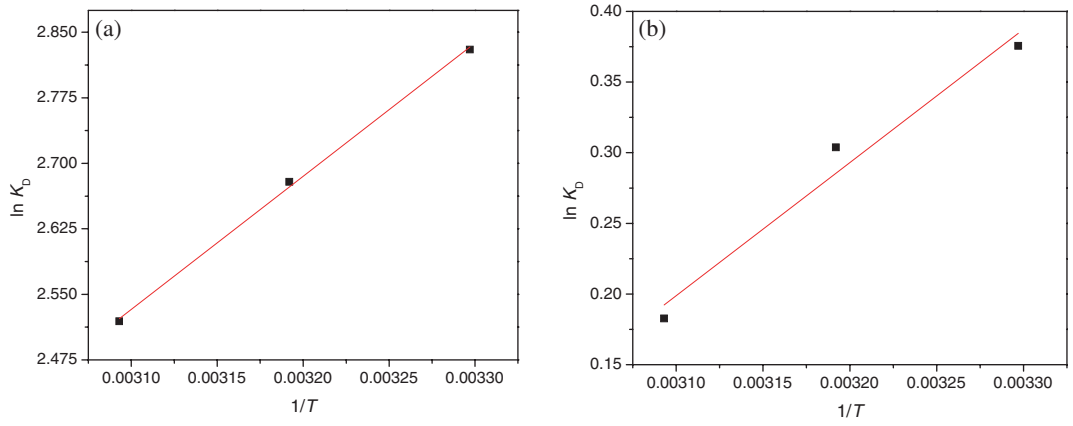

Figure 7. A plot of ln K_D against $1/T$ for the adsorption of CR by (**a**) MgAl-LDH/$CoFe_2O_4$ and (**b**) MgAl-CLDH/$CoFe_2O_4$ nanofibres.

Table 3. Values of thermodynamic parameters for CR removal with MgAl-LDH/$CoFe_2O_4$ and MgAl-CLDH/$CoFe_2O_4$ nanofibres.

Temperature (K)	$\Delta G°$ (kJ mol^{-1})	$\Delta H°$ (kJ mol^{-1})	$\Delta S°$ (J K^{-1} mol^{-1})
MgAl-LDH/$CoFe_2O_4$			
303	7.127	−12.86	−18.8926
313	6.968		
323	6.762		
MgAl-LDO/$CoFe_2O_4$			
303	−0.9459	−7.8292	−22.6707
313	−0.7905		
323	−0.4905		

from the linear regression by Langmuir and Freundlich isothermal are presented in figure 6c and e. Here, the value of correlation coefficient for the Langmuir isotherm (R^2) is larger than that of the Freundlich isotherm (R^2), which reflects that the CR covering on the MgAl-LDH/$CoFe_2O_4$ nanofibres surface is of the Langmuir type. The correlation coefficients of MgAl-CLDH/$CoFe_2O_4$ nanofibres are presented in figure 6d and f. Similar to the former, the value of correlation coefficient of MgAl-CLDH/$CoFe_2O_4$ nanofibres for the Langmuir isotherm R^2 is larger than that of the Freundlich isotherm R^2, which reflects that the CR covering on the MgAl-CLDH/$CoFe_2O_4$ nanofibres surface is also of the Langmuir type.

3.4 *Thermodynamic parameters*

The thermodynamic parameters provide in-depth information about internal energy changes that are associated with

adsorption. The thermodynamic parameters of the adsorption process such as change in standard free energy (ΔG°), enthalpy (ΔH°) and entropy (ΔS°) were obtained from experiments at various temperatures using the following equations:

$$\Delta G^\circ = -\mathrm{R}T \ln K_\mathrm{D}, \tag{7}$$

$$\ln K_\mathrm{D} = \Delta S^\circ/\mathrm{R} - \Delta H^\circ/\mathrm{R}T, \tag{8}$$

where K_D is the distribution coefficient, R the molar gas constant and T the absolute temperature. ΔH° and ΔS° of MgAl-LDH/$CoFe_2O_4$ and MgAl-CLDH/$CoFe_2O_4$ nanofibres were calculated from the slope and intercept of plots of $\ln K_\mathrm{D}$ *vs.* $1/T$ (as shown in figure 7a and b), respectively. The ΔG°, ΔH° and ΔS° values are listed in table 3. The negative values of ΔH° and ΔS° show that the adsorption process of MgAl-LDH/$CoFe_2O_4$ was exothermic with decrease in the randomness of the system. Lower free energy values (ΔG°) indicate that the process were spontaneous. The adsorption process of MgAl-CLDH/$CoFe_2O_4$ was exothermic for the negative values of ΔH° and ΔS°, which is similar to the former. Negative free energy values (ΔG°) indicate that the process is spontaneous.

4. Conclusion

In summary, we have successfully synthesized MgAl-LDH/$CoFe_2O_4$ nanofibres by urea-hydrolysed hydrothermal reaction. MgAl-LDH was well coated on the surface of $CoFe_2O_4$ and the corresponding MgAl-CLDH/$CoFe_2O_4$ nanofibres were obtained through calcination process of the MgAl-LDH/$CoFe_2O_4$ nanofibres. The nanocomposites were particularly efficient in removing CR. The kinetic studies indicated that the Langmuir model was suitable to simulate the adsorption process and the maximum adsorption amount of MgAl-LDH/$CoFe_2O_4$ nanofibres for CR was 213.2 mg g^{-1}, which was much larger than those of some other low-cost adsorbents. Therefore, these findings suggested that MgAl-LDH/$CoFe_2O_4$ nanofibres could be widely and potentially used in the field of wastewater treatment.

Acknowledgements

This work was supported by the National Natural Science Foundation of China (20907001), Training Programs of Innovation for Undergraduates of Anhui Province (AH201310360150, AH201310360279), Student Research Training Program of AHUT (2013034Y) and Outstanding Innovation Team of Anhui University of Technology (TD201202).

References

1. Shan R R, Yan L G, Yang K, Yu S J, Hao Y F, Yu H Q and Du B 2014 *Chem. Eng. J.* **252** 38
2. Ahmed I M and Gasser M S 2012 *Appl. Surf. Sci.* **259** 650
3. Lan M, Fan G L, Yang L and Li F 2014 *Ind. Eng. Chem. Res.* **53** 12943
4. Sun J C, Fan H, Nan B and Ai S Y 2014 *Sep. Purif. Technol.* **130** 84
5. Zhang Y X, Hao X D, Kuang M, Zhao H and Wen Z Q 2013 *Appl. Surf. Sci.* **283** 505
6. Chen C P, Wang P H, Lim T T, Liu L H, Liu S M and Xu R 2013 *J. Mater. Chem. A* **1** 3877
7. Werner S, Lau V W, Hug S, Duppel V, Clausen-Schaumann H and Lotsch B V 2013 *Langmuir* **29** 9199
8. Zhang H, Zhang G Y, Bi X and Chen X T 2013 *J. Mater. Chem. A* **1** 5934
9. Mi F, Chen X T, Ma Y W, Yin S T, Yuan F L and Zhang H 2011 *Chem. Commun.* **47** 12804
10. Zhang H, Hou R, Lu Z L and Duan X 2009 *Mater. Res. Bull.* **44** 2000
11. Pan D K, Zhang H, Fan T, Chen J G and Duan X 2011 *Chem. Commun.* **47** 908
12. Jia Z G, Ren D P and Zhu R S 2012 *Mater. Lett.* **66** 128
13. Zhao X R, Wang W, Zhang Y J, Wu S Z, Li F and Liu J P 2014 *Chem. Eng. J.* **250** 164
14. Hao J H, Zhang Z, Yang W S, Lu B P, Ke X, Zhang B L and Tang J L 2013 *J. Mater. Chem. A* **1** 4352
15. Layrac G, Destarac M, Gerardin C and Tichit D 2014 *Langmuir* **30** 9663
16. Das J, Patra B S, Baliarsingh N and Parida K M 2007 *J. Colloid. Inter. Sci.* **316** 216
17. Kim S J, Lee Y, Lee D K, Lee J W and Kang J K 2014 *J. Mater. Chem. A* **2** 4136
18. Bohara R A, Thorat N D, Yadav H M and Pawar S H 2014 *New J. Chem.* **38** 2979
19. Chen C P, Gunawan P and Xu R 2011 *J. Mater. Chem.* **21** 1218
20. Jacob N M, Kuruva P, Madras G and Thomas T 2013 *Ind. Eng. Chem. Res.* **52** 16384
21. Cottet L, Almeida C A P, Naidek N, Viante M F, Lopes M C and Debacher N A 2014 *Appl. Clay Sci.* **95** 25